J. Heat Mass Transfer. Vol. 17, pp. 1029–1036. Pergamon Press 1974. Printed in Great Britain

DYNAMICS OF A CROSS-FLOW HEAT EXCHANGER WITH FINS

K. WÆDE HANSEN and K. DEMANDT
Instituttet for Kemiteknik, Danmarks tekniske Højskole, Lyngby, Denmark

(*Received* 5 *June* 1973)

Abstract—Considerable temperature gradients are often found in the stationary case in the single fins of an air–water heat exchanger. A theoretical investigation of the effect of the dynamics of the fins has been performed for the over-all heat exchanger dynamics.

A model which includes radial and axial temperature profiles is compared with a simple model where radial gradients are neglected. For most practical cases it is found that the simple model represents the dynamics very well at frequencies below 10–15 rad/min.

The model for the fin is solved with high accuracy using a low order orthogonal collocation approach and the complicated 3-dimensional heat exchanger model is thus reduced to a computationally simple system.

NOMENCLATURE

A, effective heat-transfer area [m^2];
A_i, Fourier coefficient in residue expansion, equation (7);
A_r, area of tube wall [m^2];
A_{kj}, expansion coefficient in the first derivative, equation (10);
A_{fy}, outer area of heat exchanger [m^2];
A_W, area of inner tube [m^2];
B_i, Fourier coefficient in collocation expansion, equation (18);
B_{kj}, expansion coefficient in the second derivative, equation (11);
BB_{ij}, see equation (14);
C, heat content of heat exchanger and water [kcal/°C];
C_i, see equation (15);
C_p, specific heat capacity [kcal/(g°C)];
E, fin effectiveness;
$E_{1,2}$, parameters in equations (39) and (40);
F, see equation (27) [min^{-1}];
G, heat flow of air [kcal/(°C min)];
h_i, heat-transfer coefficient water–tubewall [kcal/(m^2 °C min)];
h_{y1}, heat-transfer coefficient tubewall–air [kcal/(m^2 °C min)];
h_{y2}, heat-transfer coefficient fin–air [kcal/(m^2 °C min)];
J_i, Bessel function;
K, see equation (46);
k_f, heat conductivity of fin [kcal/(m °C min)];
L, length of finned tube [m];
m, $(-s-\tau)^{1/2}$;
N, number of collocation points;
N_K, number of fins;
P_i, inner perimeter of tube [m];
P_y, outer perimeter of tube [m];
R, radius of fin [m];
R_g, UA/G;
R_{ig}, see equation (28) [min^{-1}];
R^*_{iw}, see equation (26) [min^{-1}];
R^*_W, see equation (23) [min^{-1}];
R_i, inner radius of tube [m];
R_g, outer radius of tube [m];
R_{gi}, see equation (37);
R_{gf}, see equation (38);
r', radial coordinate [m];
r, r'/R;
r_0, R_y/R;
s, $\alpha s'$;
s', Laplace parameter [min^{-1}];
T_f, temperature of fin [°C];
T_i, temperature of tube wall [°C];
T_g, temperature of air [°C];
T_W, temperature of water [°C];
T_{gi}, temperature of air before heat exchanger [°C];
T_{gu}, temperature of air after heat exchanger [°C];
T_{Wi}, temperature of water before heat exchanger [°C];
T_{Wu}, temperature of water after heat exchanger [°C];
t, time [min];
U, overall heat-transfer coefficient [kcal/(m^2 °C min)];
v_W, water flow [m^3/min];

W, heat flow of water [kcal/(°C min)];
w, fin width [m];
W_i, weight coefficient, see equation (16);
x, radial coordinate, see equation (12);
Y_i, Bessel function;
z, axial coordinate.

Greek symbols

α, $\rho_f C_{pf} R^2/k_f$ [min];
γ, pole, see equation (18);
ρ, specific weight [kg/m^3];
σ, see equation (50);
τ, $2h_y R^2/(k_f w)$;
τ_v, see equation (51);
τ_W, see equation (23);
ω, cyclic frequency.

Subscripts

f, fin;
g, air;
r, tube wall;
s, stationary;
W, water.

INTRODUCTION

THE CROSS-FLOW heat exchanger is in widespread use for air–liquid heat exchanging purposes. For example in large air-cooling systems in chemical plants and in air conditioning systems. It is the latter application which is considered in this paper, but the results have rather general validity.

The heat exchanger consists of a bundle of tubes in which the water is streaming in single or multipass arrangements. In order to obtain a high heat transfer area the tubes are normally provided with fins, which depending on the manufacture might consist of welded lamellas or whole punched plates mounted very close to each other perpendicular to the tubes. The air passes through the heat exchanger in cross-flow.

Several experimental and theoretical investigations of this system have been published in the literature (e.g. [1–3]). The investigations are based on relatively simple models, which do not take the fin-dimension into account. This does not seem very reasonable as it is wellknown that rather steep temperature profiles are often found in the fins of practical heat exchangers.

Furthermore, a recent analysis of the dynamic behaviour and control of the recirculation system [4] shows that the heat exchanger model must be valid in the high frequency domain (10–15 rad/min) to ensure a reliable stability analysis.

To clear up the dynamic effect of the heat diffusion resistance in the fin a very simple model for a fin tube is compared with a complicated model, which includes the dynamics of the fins.

The investigation is divided into two parts. First the heat diffusion in a single fin is studied and afterwards the models for the whole finned tube are compared.

HEAT TRANSPORT IN A CYLINDRICAL FIN

With the symbols given in Fig. 1 and in the notation list the following equation is derived:

$$\alpha \frac{\partial T_f}{\partial t} = \frac{1}{r}\frac{\partial}{\partial r}\left(r\frac{\partial T_f}{\partial r}\right) - \tau(T_f - T_g). \tag{1}$$

Boundary conditions:

$$T_f(0, r) = 0 \tag{2}$$

$$T_f(t, r_0) = T_i \tag{3}$$

$$\nabla T_f(t, 1) = 0. \tag{4}$$

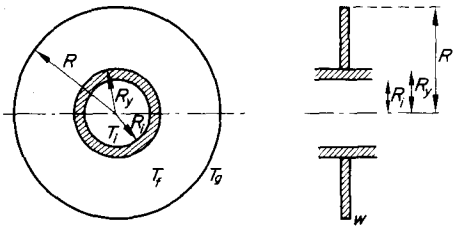

FIG. 1. Sketch of a cylindrical fin.

In these equations it is assumed that only radial temperature variations have to be considered and the heat flux through the end is negligible. These assumptions are fulfilled when the fins are thin and the thermal conductivity high.

Equations (1)–(4) are Laplace transformed giving the transfer function for disturbances in the tube temperature:

$$\frac{\overline{T}_f}{\overline{T}_i} = \frac{J_1(m)Y_0(mr) - Y_1(m)J_0(mr)}{J_1(m)Y_0(mr_0) - Y_1(m)J_0(mr_0)} \tag{5}$$

$m^2 = -s - \tau$, where s is the dimensionless Laplace parameter ($s = s'\alpha$).

J_i and Y_i are Bessel functions of order i. Integration across the fin area gives the transfer function for the mean temperature:

$$\frac{\overline{T}_{f,m}}{\overline{T}_i} = \frac{2r_0}{(1-r_0^2)m}\,\frac{Y_1(m)J_1(mr_0) - J_1(m)Y_1(mr_0)}{J_1(m)Y_0(mr_0) - Y_1(m)J_0(mr_0)}. \tag{6}$$

The impulse response can be found from (6) as the sum of residues:

$$T_{f,m}(t) = \sum_{i=1}^{\infty} \frac{A_i}{\lambda_i} e^{-\lambda_i t} \tag{7}$$

where

$$\frac{A_i}{\lambda_i} = \frac{T}{\dfrac{dN}{ds}}(s \to -\lambda_i).$$

T is the numerator and N the denominator of (6). λ_i is pole number i.

Since τ is added to the Laplace parameter s we can in the first place put $\tau = 0$ and calculate the poles as functions of r_0. In the first part of Table 1 λ_i and A_i are shown for five characteristic values or r_0. Small r_0

Table 1(a). Poles and Fourier coefficients of equation (7), $\tau = 0$

r_0	λ_1 A_1	λ_2 A_2	λ_3 A_3	λ_4 A_4	λ_5 A_5	λ_6 A_6
0·1	1·216	24·79	73·18	146·1	243·5	365·2
	1·165	0·550	0·498	0·478	0·468	0·463
0·25	2·476	37·29	107·4	212·6	353·0	528·4
	2·276	1·516	1·459	1·442	1·434	1·430
0·333	3·517	47·73	136·4	269·5	447·0	668·8
	3·168	2·340	2·281	2·264	2·257	2·253
0·5	7·407	86·34	244·2	481·1	796·9	1192·
	6·446	5·439	5·371	5·353	5·345	5·341
0·8	56·30	549·8	1537·			
	46·74	44·68	44·53			

Table 1(b). Poles and Fourier coefficients of equation (18), $\tau = 0$, $r_0 = 1/3$

N	γ_1 B_1	γ_2 B_2	γ_3 B_3	γ_4 B_4	γ_5 B_5	γ_6 B_6
1	2·995					
	2·995					
2	3·437	49·45				
	3·119	4·582				
3	3·514	48·16	166·0			
	3·167	2·062	9·284			
10	3·517	47·73	136·4	269·5	447·0	667·5
	3·168	2·340	2·281	2·265	2·234	2·603

values will give small values of λ_i and A_i. The displacement of the poles for varying τ is less for big values of r_0 than for small values and the performance of the fin will therefore not only be good but also be nearly independent of τ. This appears very clearly from

Table 2. Fin effectiveness

τ	r_0	0·1	0·25	0·333	0·5	0·8
0·5		0·72	0·84	0·89	0·95	0·99
1		0·56	0·73	0·80	0·90	0·985
2		0·40	0·59	0·67	0·81	0·97
5		0·22	0·38	0·47	0·65	0·93
10		0·15	0·26	0·33	0·49	0·87

Table 2, where the effectiveness, E, is given as a function of r_0 and τ. E is found from

$$E = \sum_{i=1}^{\infty} \frac{A_i}{\lambda_i(\tau = 0) + \tau}. \tag{8}$$

In practical heat exchangers r_0 is close to 1/3, and τ must consequently not exceed the value 2 to obtain a satisfactory effectiveness. In this region the poles are separated very much from each other, and the first pole, λ_1, will therefore dominate the response for disturbances of dimensionless frequency much less than $\lambda_2(\omega \ll \lambda_2)$. This means that a reasonable approximation to the transfer function (6) will be:

$$\frac{\overline{T}_{f,m}}{\overline{T}_i} = \frac{\lambda_1 . E}{s + \lambda_1}. \tag{9}$$

This is further illustrated below.

An approximative solution method

In this section a low order approximation of equations (1)–(4) based on orthogonal collocation is studied. This is carried out because the analytical solution method described above is lengthy and because a low order approximation based on orthogonal polynomials may be superior to truncating the series (7) after a number of terms corresponding to the approximation order.

The principles of the collocation method are described by Villadsen *et al.* in a series of publications [5–7]. Some solution possibilities when partial differential equations are solved can be found in, for example [8–11]. Very shortly the first and second derivative in collocation point k are approximated by a weighted sum of the dependent variable at the N internal collocation points and at the boundary points ($j = 1$, and $j = N+2$):

$$\frac{dT_k}{dx} = \sum_{j=1}^{N+2} A_{kj} T_j \tag{10}$$

$$\frac{d^2T_k}{dx^2} = \sum_{j=1}^{N+2} B_{kj} T_j \tag{11}$$

A and **B** are matrices with constant components and they are found once and for all for a specific polynomium type.

The radial coordinate in (1) is transformed

$$x = \frac{r - r_0}{1 - r_0} \quad (r_0 \leqslant r \leqslant 1,\ 0 \leqslant x \leqslant 1)$$

$$(1 - r_0^2)\alpha \frac{\partial T_f}{\partial t} = \frac{\partial^2 T_f}{\partial x^2} + \frac{1}{x + \dfrac{r_0}{1 - r_0}} \frac{\partial T_f}{\partial x} - (1 - r_0)^2 \tau (T_f - T_g). \tag{12}$$

After Laplace transformation and introduction of (10) and (11) in (12) and (4) the following expression is obtained:

$$\mathbf{BB} . \bar{T}_f = C \bar{T}_i \tag{13}$$

where

$$BB_{i,j} = B'_{i,j} - \frac{B'_{i,N+2}A_{N+2,j}}{A_{N+2,N+2}} - (s+\tau)(1-r_0^2).\delta_{ij} \quad (14)$$

$$C_i = -B'_{i,1} + \frac{B'_{i,N+2}A_{N+2,1}}{A_{N+2,N+2}}. \quad (15)$$

Here

$$\delta_{ij} = \begin{cases} 0 & i \neq j \\ 1 & i = j \end{cases}$$

$$B'_{i,j} = B_{i,j} + \frac{1}{x_i + \dfrac{r_0}{1-r_0}} A_{i,j}.$$

The dimensionless Laplace parameter s is only found in the diagonal of matrix **BB**. The other components are functions of the collocation constants and r_0. $\bar{T}_f$ is a vector of N components giving the temperature in the internal collocation points. The N eigenvalues of **BB** will approximately correspond to the poles in the analytical transfer function (5) or (6).

The mean temperature $\bar{T}_{f,m}$ is found from $\bar{T}_f$ through the application of quadrature formulas:

$$\begin{aligned} \bar{T}_{f,m} &= \frac{2}{1-r_0^2}\int_{r_0}^{1} \bar{T}_f r\,dr \\ &= \frac{2(1-r_0)}{1+r_0}\int_0^1 \bar{T}_f x\,dx + \frac{2r_0}{1+r_0}\int_0^1 \bar{T}_f\,dx \\ &= \frac{2}{1+r_0}\sum_{i=2}^{N+1}[(1-r_0)x_i + r_0].W_i T_{f,i}. \end{aligned} \quad (16)$$

Substitution of (13) into (16) gives:

$$\bar{T}_{f,m} = \boldsymbol{W}.\bar{T}_f = \boldsymbol{W}.(\mathbf{BB}^{-1}.\boldsymbol{C})\bar{T}_i. \quad (17)$$

Equation (17) can be transformed to a form similar to the Laplace transform of (7):

$$\frac{\bar{T}_{f,m}}{\bar{T}_i} = \sum_{j=1}^{N} \frac{B_j}{s+\gamma_j}. \quad (18)$$

For a specific value of N the first values of γ_j and B_j will correspond to the values of λ_j and A_j from the analytical solution carried through above. Later values of γ_j and B_j will not necessarily be equal to λ_j and A_j. The collocation method—roughly speaking—tries to include the influence of the modes greater than N by changing the values of λ_j and A_j for the last of the N included values.

The last half of Table 1 shows this relationship very clearly. For r_0 equal to 1/3 values of γ_j and B_j are shown for various values of N, when the collocation points have been chosen as zeros of Legendre polynomials. The most important and impressive result is that $N = 2$ gives the first two eigenvalues with high accuracy. In Fig. 2 the frequency responses are shown

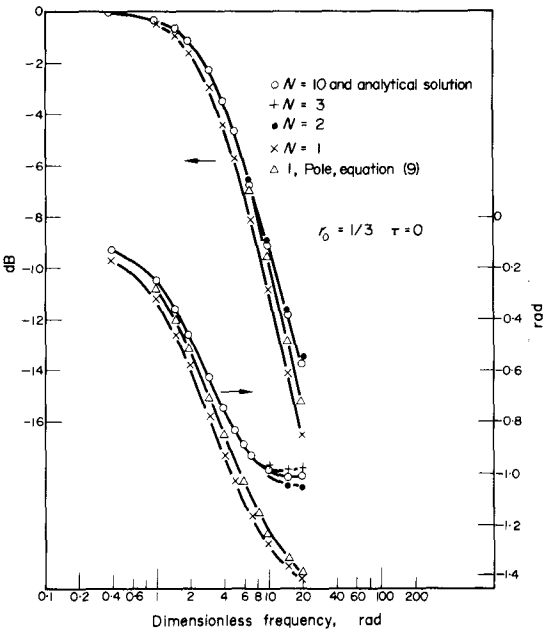

FIG. 2. Frequency response of various approximate solutions to the fin equation.

for various approximate transfer functions using $r_0 = 1/3$ and $\tau = 0$. The frequency is dimensionless. In order to change to units of rad/min one has to divide by α. Characteristic examples are:

$$\alpha = \begin{cases} 0{\cdot}08 \text{ min (aluminium, } R = 2\text{ cm}) \\ 0{\cdot}37 \text{ min (iron, } R = 1{\cdot}6\text{ cm}). \end{cases}$$

In [4] it is shown that the relevant frequency domain is $0 < \omega/\alpha < 15$ rad/min. This domain is especially in the first case displaced to the left in the figure.

It should be noticed that the collocation solution using $N = 10$ equals the analytical solution in the shown frequency interval within machine accuracy. Even the solution for $N = 2$ is satisfactory apart from very high frequencies, where small deviations in the phase curve from the true solution are found. The first order systems—the one point collocation approach and the approximation based on the first pole (9)—are also rather good. But they both have a considerable phase error at high frequencies.

It must, however, be concluded that the two point collocation approach is very satisfactory in the relevant frequency domain, and it will be used in the following to solve the fin equations in the complicated model for a whole finned tube.

HEAT TRANSFER IN A FINNED TUBE

(A) *Inclusion of the fin dimension*

A complicated model for the finned tube is derived

in the following. The most important simplifications are:

(a) A plug flow model is used for the water flow.
(b) Radial temperature gradients are neglected in the tube.
(c) No axial heat diffusion in the tube.
(d) Very thin fin material, i.e. only radial temperature gradients are considered in the fin.
(e) The air residence time is neglected.
(f) The air temperature is approximated by the average of the inlet and outlet air temperature.

This gives the following set of equations when water inlet temperature changes are considered.

Water.

$$\frac{\partial T_W}{\partial t}+\frac{1}{\tau_W}\frac{\partial T_W}{\partial z}=R_W^*(T_i-T_W) \tag{19}$$

$$T_W(t,0)=T_{Wi} \tag{20}$$

$$T_W(0,z)=0 \tag{21}$$

$$\tau_W=\frac{A_W L}{v_W} \qquad R_W^*=\frac{h_i P_i}{\rho_W C_{pW} A_W}. \tag{22, 23}$$

Tube.

$$\frac{\partial T_i}{\partial t}=R_{iw}^*(T_W-T_i)+F\nabla T_f|_{x=0}+R_{ig}(T_g-T_i) \tag{24}$$

$$T_i(0,z)=0 \tag{25}$$

$$R_{iw}^*=\frac{h_i P_i}{\rho_r C_{pr} A_r} \qquad F=\frac{k_f P_y w N_k}{(1-r_0)L\rho_r C_{pr} A_r R} \tag{26, 27}$$

$$R_{ig}=\frac{h_{y1} P_y}{\rho_r C_{pr} A_r}. \tag{28}$$

Fin.

$$(1-r_0)^2\alpha\frac{\partial T_f}{\partial t}=\frac{\partial^2 T_f}{\partial x^2}+\frac{1}{x+\dfrac{r_0}{1-r_0}}\frac{\partial T_f}{\partial x}-(1-r_0)^2\tau(T_f-T_g) \tag{12}$$

$$T_f(t,0)=T_i \tag{29}$$

$$\nabla T_f(t,1)=0 \qquad T_f(0,x)=0 \tag{30, 31}$$

$$\alpha=\frac{\rho_f C_{pf} R^2}{k_f} \qquad \tau=\frac{2h_{y2}R^2}{k_f w}. \tag{32, 33}$$

Air.

$$T_{gu}-T_{gi}=R_{gi}(T_i-T_g)+R_{gf}(T_f-T_g) \tag{34}$$

$$T_{gi}=0, \qquad T_g=(T_{gu}+T_{gi})/2=T_{gu}/2 \tag{35, 36}$$

$$R_{gi}=\frac{h_{y1}P_y(L-wN_K)}{G} \tag{37}$$

$$R_{gf}=\frac{h_{y2}[A_{fy}-P_y(L-wN_K)]}{G}. \tag{38}$$

This linear set of differential equations contain three independent variables. It was found above that the fin equation (12) could be solved by a two point collocation method with high accuracy in the relevant frequency domain. The T_f values in the collocation points and therefore also the mean temperature $T_{f,m}$ can be found explicitly as functions of T_i and T_g. Using $T_{f,m}$ instead of T_f on the right side of (34) eliminates the x-dependency from the equations, and the transfer functions can easily be derived. These algebraic manipulations are omitted because of the required space. Details can be found in [12].

The solution has the following form:

$$\frac{\overline{T}_{Wu}}{\overline{T}_{Wi}}=e^{-E_1} \tag{39}$$

$$\frac{\overline{T}_{gu,m}}{\overline{T}_{Wi}}=E_2(1-e^{-E_1}) \tag{40}$$

where E_1 and E_2 are complicated functions of the parameters and the Laplace parameter s'.

(B) *Omission of the fin dimension*

Besides the above mentioned approximations it is in this simple model assumed that the temperature of water, tube, and fins has the same value at a specific z-position:

$$\frac{\partial T_W}{\partial t}+\frac{W}{C}\frac{\partial T_W}{\partial z}=\frac{UA}{C(1+R_g/2)}(T_{gi}-T_W) \tag{41}$$

$$T_{gu}=\frac{1-R_g/2}{1+R_g/2}T_{gi}+\frac{R_g}{1+R_g/2}T_W \tag{42}$$

where $R_g=UA/G$, $W=\rho_W C_{pW} v_W$.

UA is an effective heat-transfer coefficient multiplied by the heat-transfer area. This product is determined from the parameters of the complicated model (A) giving the same static gain of the air temperature for inlet water temperature changes:

$$UA=\frac{-K}{1+K/(2G)} \tag{45}$$

$$K=W\ln\left(1-\frac{G\cdot T_{gu,m}^0}{W}\right). \tag{46}$$

C is the total heat content of heat exchanger and water:

$$C=L(\rho_W C_{pW} A_W+\rho_r C_{pr} A_r)+\rho_f C_{pf}\pi(R^2-R_y^2)wN_K \tag{47}$$

$T_{gu,m}^0$ is the static gain from equation (49) below.

From (41) and (42) the transfer functions can easily be derived:

$$\frac{\overline{T}_{Wu}}{\overline{T}_{Wi}} = e^{-\sigma} e^{-\tau v s'} \tag{48}$$

$$\frac{\overline{T}_{gu,m}}{\overline{T}_{Wi}} = \frac{W/G}{\frac{\tau_v}{\sigma} s' + 1}(1 - e^{-\sigma} e^{-\tau v s'}) \tag{49}$$

where:

$$\sigma = \frac{R_g}{\frac{W}{G}(1 + R_g/2)}, \qquad \tau_v = \frac{C}{W}. \tag{50, 51}$$

RESULTS

The two models are compared for parameters corresponding to two typical heat exchangers. In Table 3 the parameters are shown for a heat exchanger of copper with fins of aluminium (type a) and for a cast iron heat exchanger with welded fins (type b). Characteristic operating conditions are also included in the table.

Table 3

Parameter	Dimension	Type (a)	Type (b)
R_i	[m]	0·0065	0·0065
R_y	—	0·0070	0·0080
R	—	0·0210	0·0160
L	—	4·2	5·0
w	—	0·0003	0·0005
A_{fy}	[m²]	3·23	1·5
$\rho_r C_{pr}$	[kcal/(°C.m³)]	828	870
$\rho_f C_{pf}$	[kcal/(°C.m³)]	594	870
k_f	[kcal/(°C.m.min)]	3·0	0·65
h_i	[kcal/(°C.m².min)]	100	100
h_{y1}	—	2·0	2·0
h_{y2}	—	2·0	2·0
G	[kcal/(°C.min)	5·0	3·0
v_W	[m³/min]	0·0055	0·0055

Using these parameters the frequency responses are calculated and recorded in Figs. 3 and 4.

In Fig. 3, showing the result for the light heat exchanger type (a), a very fine agreement between the transfer functions (40) and (49) can be seen. Equation (48) is a simple time delay and for higher frequencies the transfer function will give a too small attenuation and too much phase delay compared with (39).

The frequency responses for the heavy heat exchanger type (b) in Fig. 4 show similar tends. But the disagreement between the models is more pronounced than in Fig. 3.

However, it must be concluded that the very simple model (B) can substitute the complicated model (A) in many cases where the accuracy especially at high frequencies is not very important.

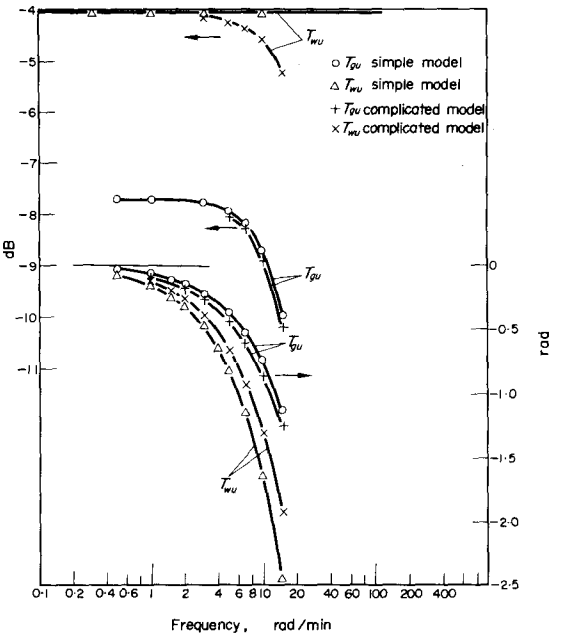

FIG. 3. Frequency responses of complicated and simplified heat exchanger models. Type (a) (see Table 3).

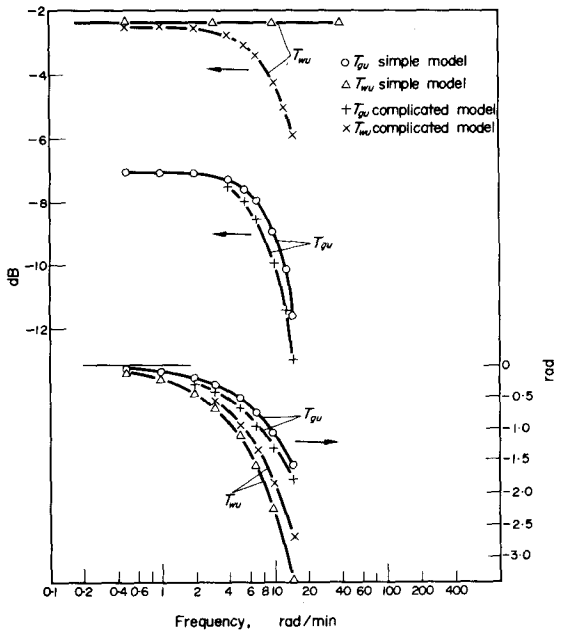

FIG. 4. As Fig. 3 for type (b).

CONCLUSION

A considerable temperature gradient is often found in the single fins of a cross-flow heat exchanger. The effectiveness of the fins is consequently less than one.

This is important for the stationary behaviour. But if this factor is included in the dynamic model Fig. 2

indicates that it is, nevertheless, possible in most cases to neglect the heat diffusion resistance in the fin.

The equation describing heat transport in a single cylindrical fin is solved very accurately using a low order orthogonal collocation method.

Two models for a whole finned tube are compared. The simple one uses the same temperature for water, tube and fin at a specific axial position, whereas the complicated one takes heat-transfer resistances between water and tube into consideration and includes heat diffusion resistance in the fins. For frequencies below 10–15 rad/min a rather good agreement between the models is obtained for heat exchangers with parameters corresponding to two quite different manufactures.

Acknowledgement—The authors would like to express their appreciation to Dr. M. L. Michelsen and Professor J. V. Villadsen for most helpful discussions.

REFERENCES

1. V. Korsgård, J. S. R. Nielsen and J. R. Jensen, The dynamic and control of the cross-flow heat exchanger (in Danish), Technical University of Denmark (1962).
2. J. R. Gartner and H. L. Harrison, Dynamic characteristics of water-to-air cross-flow heat exchangers, Presented at the Am. Soc. Heating, Refrig. and Air Cond. Engrs Meeting, Chicago (January 1965).
3. E. Bender, Dynamic responses of cross-flow heat exchangers for variations in temperature and massflow, Presented at the 5th IFAC World Congress, Paris (June 1972).
4. K. Wæde Hansen and K. Demandt, Dynamics and control of air conditioning systems (in Danish), Danish Automation Society (April 1973). (A review is going to be published.)
5. J. V. Villadsen and W. E. Stewart, Solution of boundary-value problems by orthogonal collocation, *Chem. Engng Sci.* **22**, 1483 (1967).
6. J. V. Villadsen, Selected approximation methods for chemical engineering problems, Technical University of Denmark (1970).
7. M. L. Michelsen and J. V. Villadsen, A convenient computational procedure for collocation constants, *Chem. Engng* **4**, 64 (1972).
8. J. V. Villadsen and J. P. Sørensen, Solution of parabolic partial differential equations by a double collocation method, *Chem. Engng Sci.* **24**, 1337 (1969).
9. K. Wæde Hansen, Analysis of transient models for catalytic tubular reactors by orthogonal collocation; *Chem. Engng Sci.* **26**, 1555 (1971).
10. K. Wæde Hansen, H. Livbjerg and J. V. Villadsen, Dynamic modeling of catalytic fixed-bed reactors, Presented at IFAC Symposium DISCOP, Györ, Hungary (1971).
11. K. Wæde Hansen, Simulation of the transient behaviour of a pilot plant fixed-bed reactor, *Chem. Engng Sci.* **28**, 723 (1973).
12. K. Wæde Hansen, Models for a cross-flow heat exchanger, Danish Automation Society (1972).

DYNAMIQUE D'UN ECHANGEUR DE CHALEUR A COURANTS CROISES AVEC AILETTES

Résumé—Des gradients de température considérables sont fréquemment observés, dans le cas stationnaire, pour un échangeur de chaleur air-eau à ailettes simples. On a conduit une étude théorique de l'effet des ailettes sur la dynamique générale de l'échangeur.

On compare un modèle qui inclut les profils de température radiaux et axiaux, avec un modèle simple où les gradients radiaux sont négligés. On montre que dans la plupart des cas pratiques, le modèle simple représente bien la dynamique à des fréquences inférieures à 10–15 rad/min.

On traite le modèle à ailettes avec précision en utilisant une approche à collocation orthogonale d'ordre faible et le modèle tridimensionnel est réduit à un système simple, du point de vue traitement par ordinateur.

DAS DYNAMISCHE VERHALTEN EINES BERIPPTEN KREUZSTROM-WÄRMEÜBERTRAGERS

Zusammenfassung—In den einzelnen Rippen eines Luft-Wasser-Wärmeübertragers treten im stationären Fall oft beträchtliche Temperaturgradienten auf. Über den Einfluß des dynamischen Verhaltens der Rippen auf das dynamische Verhalten des gesamten Wärmeübertragers wurde eine theoretische Untersuchung durchgeführt.

Ein Modell, das radiale und axiale Temperaturprofile enthält, wird mit einem einfachen Modell verglichen, in dem die radialen Gradienten vernachlässigt werden. Für die meisten praktischen Fälle zeigt sich, daß das einfache Modell bei Frequenzen $< (1{,}5 \div 2)\,\mathrm{min}^{-1}$ das dynamische Verhalten sehr gut wiedergibt.

Das Modell für die Rippen wird mit hoher Genauigkeit unter Benutzung einer orthogonalen Zuordnungs-Näherung niedriger Ordnung gelöst und das schwierige 3-dimensionale Wärmeübertrager-Modell wird derart auf ein berechnungsmäßig einfaches System zurückgeführt.

ДИНАМИКА ОРЕБРЕННОГО ТЕПЛООБМЕННИКА С ПОПЕРЕЧНЫМ ТЕЧЕНИЕМ

Аннотация — В стационарном случае часто обнаруживаются существенные температурные градиенты на отдельных ребрах воздушно-водяного теплообменника. Теоретически изучено влияние динамической характеристики ребер на суммарную динамическую характеристику теплообменника.

Проведено сравнение модели, учитывающей радиальные и осевые профили температуры, с простой моделью, не учитывающей радиальные градиенты температуры. В большинстве практических случаев найдено, что простая модель очень хорошо отражает динамику при частотах ниже 10–15 рад/мин.

С большой точностью получено решение для модели ребра с помощью ортогональной коллокации малого порядка и, следовательно, сложный трехмерный теплообменник сводится к простой расчетной системе.